# Studies on the Formation of Niobia in Some Aqueous Acidic Electrolytes

**ADRIAN CRISTIAN MANEA[1], LIANA ANICAI[2]***

[1] University Politehnica of Bucharest, Faculty of Applied Chemistry and Material Sciences, Department of Inorganic Chemistry, Physical Chemistry and Electrochemistry, 1-7 Polizu Str., 011061, Bucharest, Romania

[2] University Pilotehnica of Bucharest, Center for Surface Science and Nanotechnology, 313 Splaiul Independentei, 060042, Bucharest, Romania

*Chemical and electrochemical formation of oxide films on Nb in aqueous oxalic, sulfuric and nitric acids, at concentrations of 0.1-0.5 M in galvanostatic mode at different current densities and up to certain formation potential values, was studied. The influence of formation potential, applied current density and chemical nature of the involved electrolyte during passivation on the stability and behaviour of oxide film capacitance, were also studied. Experimental data obtained using electrochemical impedance spectroscopy technique were modeled using corresponding equivalent electrical circuits.*

*Keywords: niobia, native oxide, anodic oxidation, electrochemical impedance spectroscopy, equivalent circuits*

In recent years, there is a tendency to replace the tantalum oxide, with niobium oxide (niobia, as $NbO_2$, or $Nb_2O_5$) as a dielectric material for capacitors [1], as its dielectric constant ($\varepsilon_r = 41$) is higher than that of the tantalum oxide ($\varepsilon_r = 23\text{-}27$). In addition, niobia layers are involved in optoelectronic applications, including the building of solar cells, due to their good electrochromic and photo-electrochemical properties.

To form niobium oxide films, the anodic oxidation of niobium metal is usually involved, as a cost-effective route which may provide various morphologies, including ordered porous nanostructures. We notice that few papers were published about this subject. Choi et al. [2] reported the formation of anodic niobium oxide in mixtures of HF and $H_3PO_4$, aqueous solutions emphasizing choice of this electrolyte in terms of the preparation of pores without dissolution of the surface of the formed oxide. They found that the single HF electrolyte leads to the formation of pores as well as to their destruction by the dissolution of pore wall, whereas the dissolution of the formed oxide is significantly retarded by the addition of appropriate amount of $H_3PO_4$. The authors also concluded that the interpore distance of porous niobium oxide is determined by anodization potential with a growth rate of 1.4 nm/V, similar with that reported in the preparation of porous alumina. Skatov et al. [3] investigated anodic crystalline niobium oxide involving 1 M $H_2SO_4$ electrolyte, with the addition of various HF concentrations (0.5 – 2 M). These authors took into consideration the wide range of Nb valence states due to the incomplete configurations of d-electrons, which may led to the presence of low valence oxides, mainly located at the metal/high valence oxide boundary. They showed that during Nb anodization in the absence of the activator (in this case HF) the current practically did not depend on potential; thus, the anodic oxide film of the barrier type that had an amorphous structure was formed on niobium.

## Experimental part

The measurements were carried out using a conventional three-electrode electrochemical cell. The used working electrode was made of a cylindrical pellet of niobium of 99.9% purity (Goodfellow) with an exposed surface area of 3.14 $mm^2$. A platinum mesh was used as auxiliary electrode. Electrode potentials were measured against Ag/AgCl reference electrode in saturated KCl. Aqueous solutions of oxalic, sulfuric and nitric acid having concentrations in the range of 0.1 – 0.5 M have been used as electrolytes and they have been prepared using reagent-grade chemicals (Merck) and Millipore water (with a conductivity of about 18.2 MΩ.cm). Before each determination, the Nb working electrode was polished using 0.05 μm alumina suspension (Leco), then thoroughly washed with water and dried.

All electrochemical experiments have been performed using a PGSTAT 12 (Metrohm Autolab) electrochemical system. Electrochemical impedance spectra (EIS) were measured at room temperature (23 ± 2°C), at the open circuit potential in the frequency range 1 MHz - 0.05 Hz, overlapping with a 10 mV amplitude a.c. signal. Experimental data were modelled using corresponding equivalent electrical circuits and the values of circuit component were obtained using ZView 3.1 software (Scribner Inc.).

## Results and discussions

*The chemical formation and behavior of native niobia*

For the growth of the native niobia studies, the electrode was immersed in the investigation solution and the open-circuit potential against time was recorded. The increase of the chemically pure native oxide film practically occurs in the first 5-10 min , for all solutions, as shown in figure 1.

Then, the formed native film has been characterized in the same solution, through a series of EIS spectra recorded at open circuit potential, in steps of 15 min. From these spectra, oxide resistance ($R_{ox}$) and oxide capacitance ($C_{ox}$) parameters from the proposed equivalent circuit to model the experimental data were obtained.

Open-circuit potential curves (fig. 2) illustrate passive behavior of native niobia. EIS spectra of native film growth during two hours show capacitive features virtually identical for all forming potential for all solutions of acids

* email: lanicai@itcnet.ro

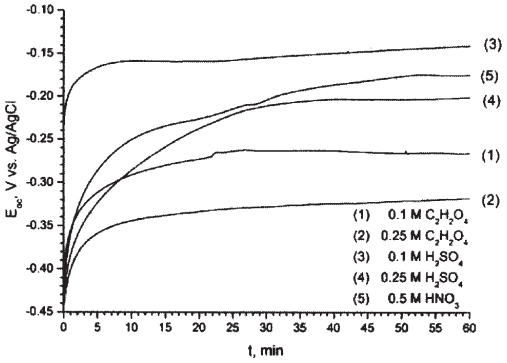


Fig. 1. The open-circuit potential dependence against time for native niobia, in various acid solutions

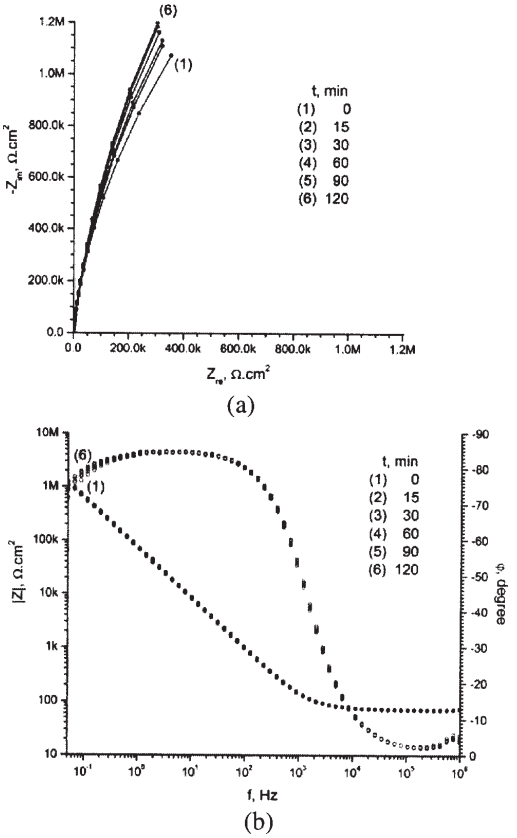


Fig. 2. Nyquist (a) and Bode (b) (● - impedance modulus (|Z|); o - phase angle (φ)) representations of EIS spectra for native niobia in 0.1 M $H_2SO_4$.

used. Impedance modulus is kept constant at high frequency in a wide range. Differences occur in the spectra of native niobia formed in oxalic acid solutions, when semicircles are depressed and well defined. For the other two types of electrolytes (based on sulfuric and nitric acids) the recorded spectra present an arc close to the vertical axis, proving the formation of a solid electrically insulating film.

The proposed equivalent circuit model of $Nb/Nb_2O_5$/electrolyte interface is shown in figure 3, which is a general model of valve metal oxide interface. In this model, $R_s$ is the ohmic resistance of the solution, $CPE_{ox}$ and $R_{ox}$ represent the total capacity of the oxide film (expressed as a constant phase element) and, respectively, the total resistance of the oxide film. We mention that an identical circuit was chosen for the formation of zirconium oxide [4].

Figure 4 shows the dependence against immersion time of impedance modulus (|Z|), respectively of $R_{ox}$·$C_{ox}$ time-constant for the native niobia.

As illustrated in figure 4, except for the initial 30 minutes, the impedance modulus remains practically constant over

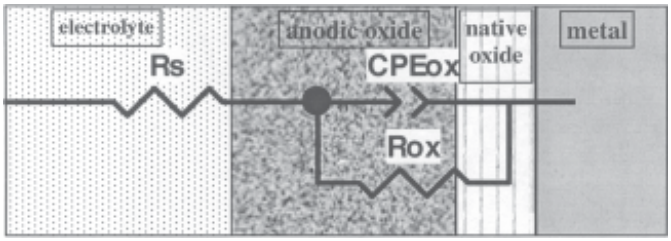


Fig. 3. Equivalent circuit model of $Nb/Nb_2O_5$/electrolyte interface

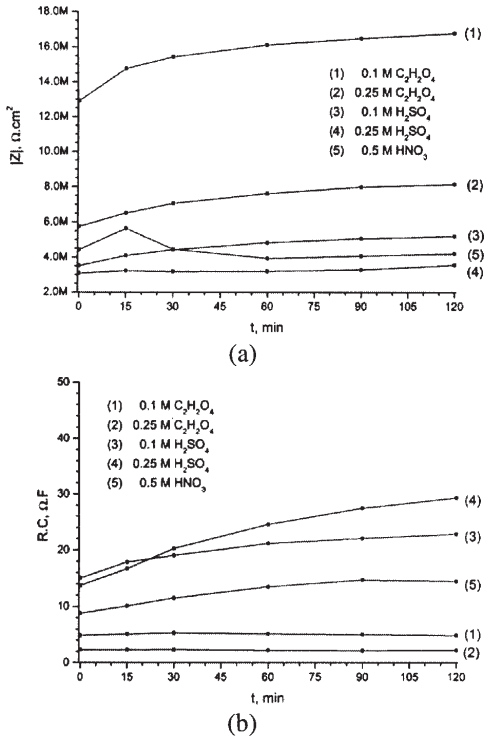


Fig. 4. Dependence of |Z| (a) and time-constant (b) against time for native niobia, in the investigated solutions

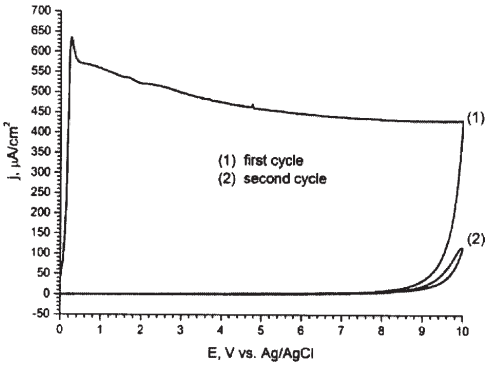


Fig. 5. Cyclic voltammetry curves of Nb electrode in 0.1 M $C_2H_2O_4$ electrolyte at successive scans (v = 100 $mVs^{-1}$)

time; however it has different values depending on the chemical nature and the concentration of acid solution. The highest recorded value was evidenced in the case of 0.1 M oxalic acid, probably due to the slow growth of the film. During immersion of the electrode, the film becomes more compact, with an uniform structure. In the same time the low acid concentration does not determine a significant dissolution of the oxide over time.

The oxide films grown in strong acids (sulfuric and nitric) had quite similar values, but significantly lower than those obtained in the case of oxalic acid solutions. This behaviour may suggest the presence of a dynamic balance between thickness increase and dissolution due to the acidic solution chemical attack.

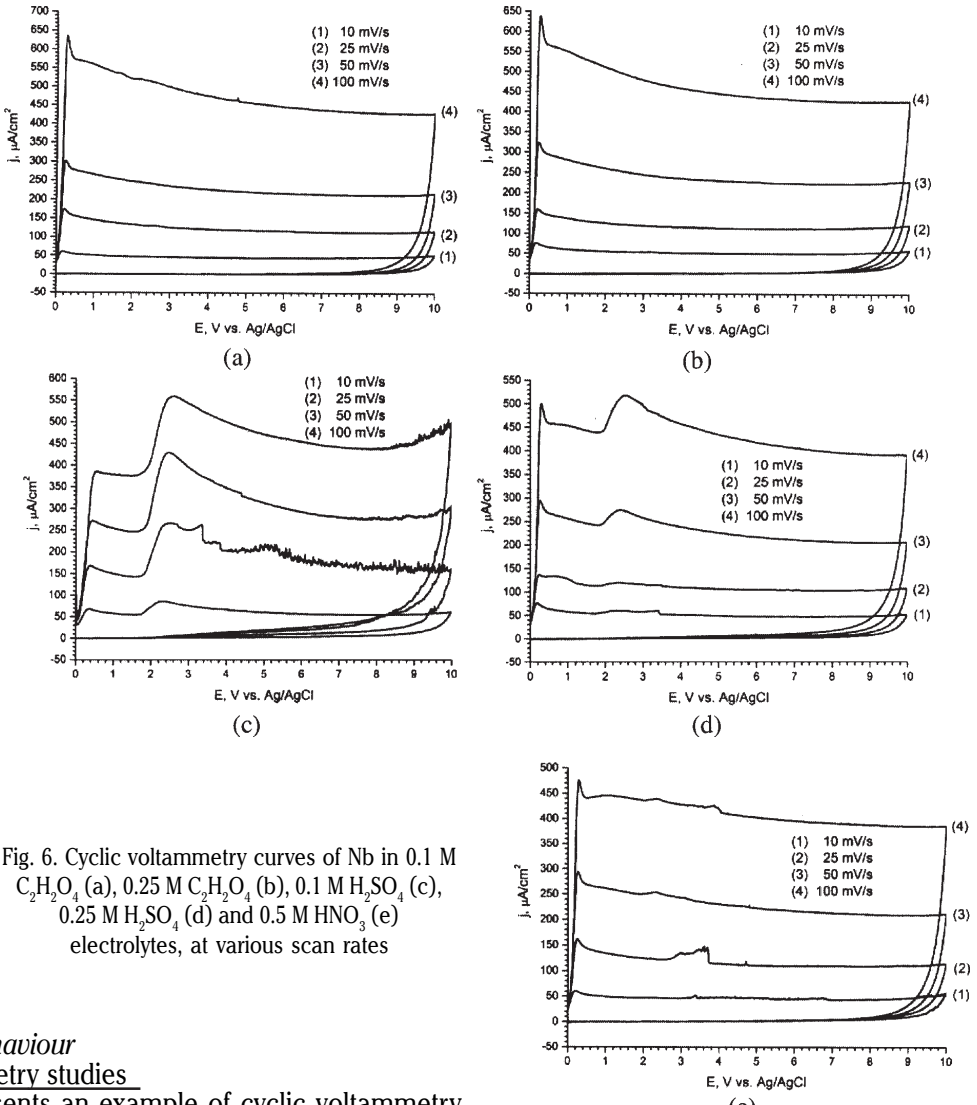


Fig. 6. Cyclic voltammetry curves of Nb in 0.1 M $C_2H_2O_4$ (a), 0.25 M $C_2H_2O_4$ (b), 0.1 M $H_2SO_4$ (c), 0.25 M $H_2SO_4$ (d) and 0.5 M $HNO_3$ (e) electrolytes, at various scan rates

*Anodic films behaviour*

Cyclic voltammetry studies

Figure 5 presents an example of cyclic voltammetry curves (recorded from 0.1 M oxalic acid solution), which are characteristic of the formation of electric insulating anodic film.

In figure 6(a-e), the first cycle of recorded voltammograms at different scanning rates (10-100 $mVs^{-1}$ is presented, corresponding to the different electrolysis media. The figures show that voltammograms exhibit almost the same shape, for all applied scan rates and investigated electrolytes.

Unlike the oxalic and nitric acids based electrolytes, sulfuric acid solutions determine the appearance of a second region on the voltammogram at about 2-3 V/AgCl anodization as figures 6 (c,d) show. In this medium, the current jumps to the second region become broader as the concentration increased from 0.1 M to 0.25 M. This phenomenon might suggest a transition of the niobium oxidation state, namely the gradual oxidation of the niobium to the $NbO_2$ and $Nb_2O_5$, the last being the stable form of niobia. Diluted sulfuric acid solution also leads to a higher concentration of niobium oxide intermediate (tetravalent niobium oxide). Therefore, one can assume that the oxalic and nitric acids based solution facilitates the growth of the anodic layer in a single step by the direct oxidation to the maximum valence of the niobium, resulting $Nb_2O_5$.

We noticed that the anodic current density proportionally increased with the applied potential scan rate for all the investigated solutions.

The influence of anodizing potential on the stability of passive films

To study the influence of the anodizing potential ($E_f$) on the stability of niobium oxide passive films the inverse capacitance dependence against time, obtained for each of the test solutions at all applied current densities (j) and formation potentials was analyzed, an example being shown in figure 7 for 0.1 M $C_2H_2O_4$. Linear dependences of the reciprocal capacitance - time dependence, $C^{-1} = a + b \cdot t$, with a and b parameters that depend on the electrical charge ($Q_a$) for anodic process were obtained. Tables 1-5 present the calculated results for all investigated solutions and applied current density values. A value for $\varepsilon_r$ equal to 41 was used [5].

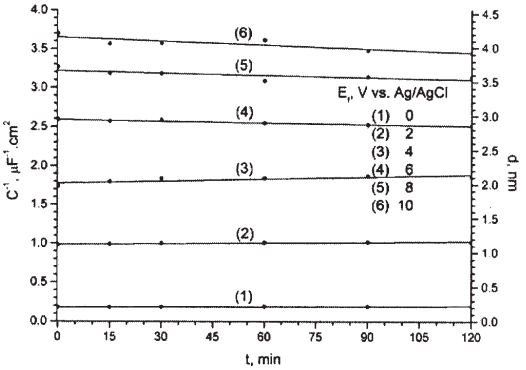


Fig. 7. Both reciprocal capacitance and film thickness vs. time dependence in 0.1 M $C_2H_2O_4$ electrolyte (for current density j = 0.5 $mAcm^{-2}$)

**Table 1**
VALUES OF PARAMETERS IN THE RECIPROCAL CAPACITANCE - TIME DEPENDENCE ($C^{-1} = a + b \cdot t$)

| j, mA·cm$^{-2}$ | $E_f$, V vs. Ag/AgCl | $Q_a$, mC | a , μF$^{-1}$cm$^2$ | b · 10$^4$, μF$^{-1}$ cm$^2$min$^{-1}$ |
|---|---|---|---|---|
| 0 | - | - | 0.18 | 1.31 |
| 0.5 | 2 | 0.87 | 0.99 | 2.76 |
| | 4 | 2.18 | 1.77 | 8.72 |
| | 6 | 2.84 | 2.59 | -7.07 |
| | 8 | 3.17 | 3.22 | -9.85 |
| | 10 | 3.66 | 3.65 | -17.20 |
| 1.0 | 2 | 0.88 | 0.96 | 1.26 |
| | 4 | 1.65 | 1.95 | 6.06 |
| | 6 | 2.75 | 2.49 | 2.52 |
| | 8 | 2.76 | 3.16 | 5.37 |
| | 10 | 3.10 | 3.44 | 8.15 |
| 2.5 | 2 | 0.75 | 0.73 | 2.65 |
| | 4 | 1.40 | 1.73 | 5.11 |
| | 6 | 2.19 | 2.50 | 5.93 |
| | 8 | 2.33 | 2.96 | 7.79 |
| | 10 | 2.72 | 3.59 | 9.40 |

**Table 2**
VALUES OF PARAMETERS IN THE RECIPROCAL CAPACITANCE - TIME DEPENDENCE ($C^{-1} = a + b \cdot t$) FOR Nb ELECTRODE IN 0.25 M $C_2H_2O_4$ ELECTROLYTE AT DIFFERENT CHARGES OF FILM FORMATION

| j, mA·cm$^{-2}$ | $E_f$, V vs. Ag/AgCl | $Q_a$, mC | a , μF$^{-1}$cm$^2$ | b · 10$^4$, μF$^{-1}$ cm$^2$min$^{-1}$ |
|---|---|---|---|---|
| 0 | - | - | 0.18 | 2.58 |
| 0.5 | 2 | 0.89 | 0.96 | 0.55 |
| | 4 | 1.76 | 1.86 | -3.48 |
| | 6 | 2.07 | 2.88 | -0.53 |
| | 8 | 2.73 | 3.15 | -5.57 |
| | 10 | 3.66 | 4.34 | 6.57 |
| 1.0 | 2 | 0.86 | 0.91 | -0.10 |
| | 4 | 1.45 | 1.63 | 1.28 |
| | 6 | 1.98 | 2.11 | -3.73 |
| | 8 | 2.64 | 2.03 | -8.93 |
| | 10 | 3.21 | 3.09 | -10.60 |
| 2.5 | 2 | 0.75 | 0.73 | 3.61 |
| | 4 | 1.41 | 1.24 | 2.08 |
| | 6 | 1.89 | 1.40 | 2.08 |
| | 8 | 2.27 | 2.49 | -7.72 |
| | 10 | 2.60 | 2.84 | -6.52 |

**Table 3**
VALUES OF PARAMETERS IN THE RECIPROCAL CAPACITANCE - TIME DEPENDENCE ($C^{-1} = a + b \cdot t$) FOR Nb ELECTRODE IN 0.1 M $H_2SO_4$ ELECTROLYTE AT DIFFERENT CHARGES OF FILM FORMATION

| j, mA·cm$^{-2}$ | $E_f$, V vs. Ag/AgCl | $Q_a$, mC | a , μF$^{-1}$cm$^2$ | b · 10$^4$, μF$^{-1}$ cm$^2$min$^{-1}$ |
|---|---|---|---|---|
| 0 | - | - | 0.34 | 1.59 |
| 0.5 | 2 | 0.45 | 1.62 | -1.13 |
| | 4 | 1.23 | 2.25 | 7.71 |
| | 6 | 2.28 | 2.90 | 12.90 |
| | 8 | 2.79 | 3.37 | 5.88 |
| | 10 | 3.29 | 4.26 | 21.90 |
| 1.0 | 2 | 0.41 | 1.09 | 6.09 |
| | 4 | 1.41 | 2.32 | -2.24 |
| | 6 | 5.10 | 3.28 | -4.67 |
| | 8 | 2.17 | 4.02 | -14.40 |
| | 10 | 3.81 | 4.63 | -10.10 |
| 2.5 | 2 | 0.41 | 0.94 | 5.71 |
| | 4 | 0.69 | 1.57 | 8.39 |
| | 6 | 1.72 | 2.69 | 2.90 |
| | 8 | 1.81 | 3.50 | 4.89 |
| | 10 | 2.03 | 3.95 | 4.94 |

The influence of the applied current density value on the stability of passive films

In order to study the influence of the applied current density on growth and stability of the anodic niobium oxide films, the inverse capacitance dependence against time, obtained for each of the test solutions at a formation constant potential of 10 V vs. Ag/AgCl was analyzed, an example being presented in figure 8. Table 6 presents the calculated results for all studied solutions and current density values.

**Table 4**
VALUES OF PARAMETERS IN THE RECIPROCAL CAPACITANCE - TIME DEPENDENCE ($C^{-1} = a + b \cdot t$) FOR Nb ELECTRODE IN 0.25 M $H_2SO_4$ ELECTROLYTE AT DIFFERENT CHARGES OF FILM FORMATION

| j, mA·cm$^{-2}$ | $E_f$, V vs. Ag/AgCl | $Q_a$, mC | a , μF$^{-1}$cm$^2$ | b · 10$^4$, μF$^{-1}$ cm$^2$min$^{-1}$ |
|---|---|---|---|---|
| 0 | - | - | 0.19 | 0.53 |
| 0.5 | 2 | 0.80 | 1.11 | -0.87 |
| | 4 | 1.54 | 2.37 | -1.67 |
| | 6 | 2.94 | 2.84 | -0.67 |
| | 8 | 2.96 | 3.48 | 6.31 |
| | 10 | 3.63 | 4.71 | 16.90 |
| 1.0 | 2 | 0.66 | 0.91 | -0.10 |
| | 4 | 1.46 | 1.63 | 1.28 |
| | 6 | 2.17 | 2.11 | -3.73 |
| | 8 | 2.54 | 2.03 | -8.93 |
| | 10 | 2.25 | 3.09 | -10.60 |
| 2.5 | 2 | 0.68 | 0.70 | 1.53 |
| | 4 | 1.26 | 1.58 | 6.07 |
| | 6 | 1.63 | 2.94 | 10.20 |
| | 8 | 2.12 | 3.37 | 8.00 |
| | 10 | 2.43 | 3.76 | 14.50 |

**Table 5**
VALUES OF PARAMETERS IN THE RECIPROCAL CAPACITANCE - TIME DEPENDENCE ($C^{-1} = a + b \cdot t$) FOR Nb ELECTRODE IN 0.5 M $HNO_3$ ELECTROLYTE AT DIFFERENT CHARGES OF FILM FORMATION

| j, mA·cm$^{-2}$ | $E_f$, V vs. Ag/AgCl | $Q_a$, mC | a , μF$^{-1}$cm$^2$ | b · 10$^4$, μF$^{-1}$ cm$^2$min$^{-1}$ |
|---|---|---|---|---|
| 0 | - | - | 0.28 | 1.46 |
| 0.5 | 2 | 0.71 | 5.69 | 3.43 |
| | 4 | - | - | - |
| | 6 | - | - | - |
| | 8 | - | - | - |
| | 10 | - | - | - |
| 1.0 | 2 | 0.74 | 0.81 | 1.77 |
| | 4 | - | - | - |
| | 6 | - | - | - |
| | 8 | - | - | - |
| | 10 | - | - | - |
| 2.5 | 2 | 0.69 | 0.57 | 1.21 |
| | 4 | 1.88 | 2.30 | -3.62 |
| | 6 | 2.87 | 2.43 | -2.32 |
| | 8 | 2.50 | 4.22 | 2.68 |
| | 10 | 3.25 | 4.70 | -5.46 |

The influence of passivation medium on the stability of passive films

In order to study the effect of current density on formation and stability of niobia films, the inverse capacitance against time at $E_f$ = 2 V vs Ag/AgCl (for 0.25 M $C_2H_2O_4$, 0.25 M $H_2SO_4$ and 0.5 M $HNO_3$ solutions) was shown in figure 9. Table 7 presents the calculated results for all studied solutions and current density values.

Modeling of the experimental data for niobium electrode

The equivalent electrical circuit showed in figure 3 was used to obtain the solution ohmic resistance values ($R_s$), the values of the oxide film resistance ($R_{ox}$) and the parameters of the constant phase element ($Q_{ox}$ and $n_{ox}$) from experimental data. Knowing the values of the native oxide film capacity (chemical film) and calculating the oxide film capacity ("real" film capacity, $C_{ox}$, according to the ref. [6]), the anodic oxide film capacitance and the thickness of the anodic film ($d_a$) can be estimated (tables 8-12).

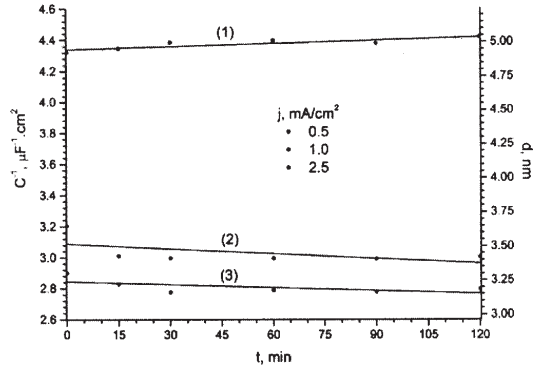


Fig. 8. The reciprocal capacitance - time dependences in 0.1 M $C_2H_2O_4$ electrolyte for various current densities at $E_f$ = +10 V vs. Ag/AgCl

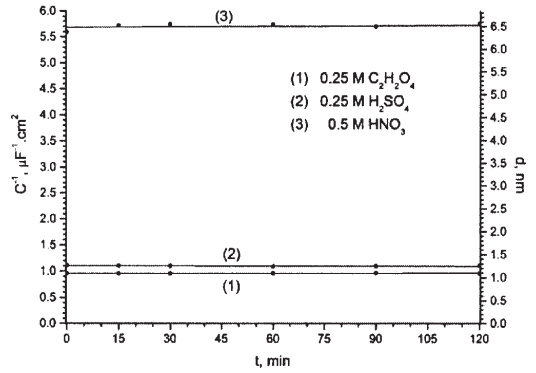


Fig. 9. The reciprocal capacitance - time dependences in various electrolytes at j = 0.5 mAcm$^{-2}$ ($E_f$ = +2 V vs. Ag/AgCl)

**Table 6**
VALUES OF PARAMETERS IN THE RECIPROCAL CAPACITANCE - TIME DEPENDENCE ($C^{-1} = a + b \cdot t$) FOR Nb ELECTRODE POLARIZED AT +10 V FORMATION POTENTIAL IN VARIOUS ELECTROLYTES

| media | j, mA·cm$^{-2}$ | $Q_a$, mC | a , μF$^{-1}$cm$^2$ | b · 10$^4$, μF$^{-1}$ cm$^2$min$^{-1}$ |
|---|---|---|---|---|
| 0.1 M $H_2C_2O_4$ | 0.5 | 3.66 | 3.65 | -17.20 |
| | 1.0 | 3.10 | 3.44 | 8.15 |
| | 2.5 | 2.72 | 3.59 | 9.40 |
| 0.25 M $H_2C_2O_4$ | 0.5 | 3.66 | 4.34 | 6.57 |
| | 1.0 | 3.21 | 3.09 | -10.60 |
| | 2.5 | 2.60 | 2.84 | -6.52 |
| 0.1 M $H_2SO_4$ | 0.5 | 3.29 | 4.26 | 21.90 |
| | 1.0 | 3.81 | 4.63 | -10.10 |
| | 2.5 | 2.03 | 3.95 | 4.94 |
| 0.25 M $H_2SO_4$ | 0.5 | 3.63 | 4.71 | 16.90 |
| | 1.0 | 2.25 | 4.79 | 5.69 |
| | 2.5 | 2.43 | 3.76 | 14.50 |
| 0.5 M $HNO_3$ | 0.5 | - | 5.69 | 3.43 |
| | 1.0 | - | 0.81 | 1.77 |
| | 2.5 | 3.25 | 0.57 | 1.21 |

**Table 7**
VALUES OF PARAMETERS IN THE RECIPROCAL CAPACITANCE - TIME DEPENDENCE ($C^{-1} = a + b \cdot t$) FOR NB ELECTRODE POLARIZED AT +2 V FORMATION POTENTIAL IN VARIOUS ELECTROLYTES

| j, mAcm$^{-2}$ | Electrolyte type and concentration | $Q_a$, mC | a , μF$^{-1}$cm$^2$ | b · 10$^4$, μF$^{-1}$ cm$^2$min$^{-1}$ |
|---|---|---|---|---|
| 0.5 | $H_2C_2O_4$ 0.25M | 0.89 | 0.96 | 0.55 |
| | $H_2SO_4$ 0.25M | 0.80 | 1.11 | -0.87 |
| | $HNO_3$ 0.5M | 0.71 | 5.69 | 3.43 |
| 1.0 | $H_2C_2O_4$ 0.25M | 0.86 | 0.91 | -0.10 |
| | $H_2SO_4$ 0.25M | 0.66 | 0.67 | 2.22 |
| | $HNO_3$ 0.5M | 0.74 | 0.81 | 1.77 |
| 2.5 | $H_2C_2O_4$ 0.25M | 0.75 | 2.84 | -6.52 |
| | $H_2SO_4$ 0.25M | 0.68 | 3.76 | 14.50 |
| | $HNO_3$ 0.5M | 0.69 | 4.70 | -5.46 |

| j, mA | $E_f$, V | $Q_a$, mC | $R_s$, Ω | $R_{ox}$, MΩ | $Q_{ox}$·10$^8$, Ω$^{-1}$s$^{-n}$ | $n_{ox}$ | $C_{ox}$, nF | $C_a$, nF | $d_{ox}$, nm | $d_a$, nm |
|---|---|---|---|---|---|---|---|---|---|---|
| 0 | - | - | 124.20 | 0.87 | 504.10 | 0.931 | 5587.20 | - | 0.20 | - |
| 0.5 | 2 | 0.87 | 120.30 | 18.41 | 87.15 | 0.945 | 1019.70 | 1247.35 | 1.12 | 0.91 |
| | 4 | 2.18 | 120.00 | 23.10 | 48.85 | 0.934 | 576.69 | 643.07 | 1.98 | 1.77 |
| | 6 | 2.84 | 120.60 | 24.07 | 34.57 | 0.949 | 386.03 | 414.68 | 2.95 | 2.75 |
| | 8 | 3.17 | 120.30 | 39.58 | 26.48 | 0.940 | 306.18 | 323.93 | 3.72 | 3.52 |
| | 10 | 3.66 | 117.70 | 18.12 | 24.00 | 0.920 | 270.33 | 284.08 | 4.21 | 4.01 |
| 1.0 | 2 | 0.88 | 119.50 | 23.92 | 89.14 | 0.949 | 1048.66 | 1290.95 | 1.09 | 0.88 |
| | 4 | 1.65 | 116.90 | 24.14 | 45.64 | 0.942 | 526.98 | 581.86 | 2.16 | 1.96 |
| | 6 | 2.75 | 114.80 | 20.82 | 35.66 | 0.931 | 411.26 | 443.93 | 2.77 | 2.57 |
| | 8 | 2.76 | 120.40 | 28.28 | 27.95 | 0.937 | 319.42 | 338.79 | 3.57 | 3.36 |
| | 10 | 3.10 | 118.40 | 25.92 | 25.43 | 0.917 | 299.22 | 316.15 | 3.81 | 3.60 |
| 2.5 | 2 | 0.75 | 117.90 | 19.91 | 11.48 | 0.941 | 1390.20 | 1850.68 | 0.82 | 0.62 |
| | 4 | 1.40 | 119.50 | 23.31 | 48.74 | 0.932 | 577.98 | 644.67 | 1.97 | 1.77 |
| | 6 | 2.19 | 115.70 | 30.37 | 34.91 | 0.938 | 406.56 | 438.47 | 2.80 | 2.60 |
| | 8 | 2.33 | 116.60 | 23.98 | 29.57 | 0.924 | 345.21 | 367.95 | 3.30 | 3.10 |
| | 10 | 2.72 | 115.60 | 22.01 | 24.18 | 0.909 | 282.85 | 297.93 | 4.03 | 3.82 |

**Table 8**
THE VALUES OF CIRCUIT PARAMETERS AND ANODIC LAYER THICKNESSES OBTAINED FROM 0.1 M $C_2H_2O_4$ ELECTROLYTE USING EIS DATA

| j, mA | $E_f$, V | $Q_a$, mC | Rs, Ω | $R_{ox}$, MΩ | $Q_{ox}$·10$^8$, Ω$^{-1}$s$^{-n}$ | $n_{ox}$ | $C_{ox}$, nF | $C_a$, nF | $d_{ox}$, nm | $d_a$, nm |
|---|---|---|---|---|---|---|---|---|---|---|
| 0 | - | - | 66.60 | 0.40 | 545.34 | 0.932 | 5736.06 | - | 0.20 | - |
| 0.5 | 2 | 0.89 | 67.53 | 12.86 | 91.22 | 0.946 | 1044.98 | 1277.75 | 1.09 | 0.89 |
| | 4 | 1.76 | 70.22 | 32.58 | 46.87 | 0.953 | 534.57 | 589.51 | 2.13 | 1.93 |
| | 6 | 2.07 | 70.12 | 23.62 | 30.78 | 0.943 | 345.96 | 368.17 | 3.29 | 3.09 |
| | 8 | 2.73 | 72.73 | 34.60 | 27.37 | 0.940 | 314.20 | 332.41 | 3.63 | 3.43 |
| | 10 | 3.66 | 72.41 | 19.57 | 20.95 | 0.930 | 231.38 | 241.11 | 4.92 | 4.73 |
| 1.0 | 2 | 0.86 | 70.81 | 21.13 | 95.66 | 0.955 | 1099.80 | 1360.69 | 1.04 | 0.84 |
| | 4 | 1.45 | 71.06 | 23.14 | 52.25 | 0.942 | 606.96 | 678.78 | 1.88 | 1.68 |
| | 6 | 1.98 | 69.90 | 20.78 | 40.07 | 0.935 | 461.64 | 502.05 | 2.47 | 2.27 |
| | 8 | 2.64 | 72.53 | 27.91 | 40.43 | 0.933 | 478.82 | 522.43 | 2.38 | 2.18 |
| | 10 | 3.21 | 73.93 | 18.36 | 27.65 | 0.927 | 312.16 | 330.13 | 3.65 | 3.45 |
| 2.5 | 2 | 0.75 | 75.00 | 9.57 | 120.66 | 0.942 | 1397.95 | 1848.44 | 0.82 | 0.62 |
| | 4 | 1.41 | 77.51 | 25.38 | 68.61 | 0.945 | 806.03 | 937.81 | 1.41 | 1.21 |
| | 6 | 1.89 | 77.50 | 18.14 | 59.57 | 0.929 | 709.98 | 810.27 | 1.60 | 1.41 |
| | 8 | 2.27 | 77.58 | 16.83 | 34.35 | 0.931 | 389.11 | 417.43 | 2.93 | 2.73 |
| | 10 | 2.60 | 79.71 | 20.19 | 29.95 | 0.924 | 344.90 | 366.97 | 3.30 | 3.10 |

**Table 9**
THE VALUES OF CIRCUIT PARAMETERS AND ANODIC LAYER THICKNESSES OBTAINED FROM 0.25 M $C_2H_2O_4$ ELECTROLYTE USING EIS DATA

| j, mA | $E_f$, V | $Q_a$, mC | Rs, Ω | $R_{ox}$, MΩ | $Q_{ox}\cdot10^8$, $\Omega^{-1}s^{-n}$ | $n_{ox}$ | $C_{ox}$, nF | $C_a$, nF | $d_{ox}$, nm | $d_a$, nm |
|---|---|---|---|---|---|---|---|---|---|---|
| 0 | - | - | 71.62 | 5.06 | 252.29 | 0.938 | 2969.64 | - | 0.38 | - |
| 0.5 | 2 | 0.45 | 71.55 | 26.03 | 53.00 | 0.947 | 611.76 | 770.49 | 1.86 | 1.48 |
| | 4 | 1.23 | 59.11 | 78.56 | 38.27 | 0.954 | 449.54 | 529.73 | 2.53 | 2.15 |
| | 6 | 2.28 | 59.04 | 75.14 | 30.08 | 0.954 | 348.87 | 395.31 | 3.27 | 2.88 |
| | 8 | 2.79 | 58.54 | 83.02 | 24.44 | 0.941 | 293.74 | 325.98 | 3.88 | 3.50 |
| | 10 | 3.29 | 58.41 | 141.06 | 18.64 | 0.936 | 231.58 | 251.17 | 4.92 | 4.54 |
| 1.0 | 2 | 0.41 | 72.07 | 24.37 | 74.79 | 0.930 | 925.31 | 1344.12 | 1.23 | 0.85 |
| | 4 | 1.41 | 71.94 | 33.85 | 37.06 | 0.944 | 428.61 | 500.90 | 2.66 | 2.27 |
| | 6 | 5.10 | 69.07 | 33.97 | 25.96 | 0.933 | 301.97 | 336.15 | 3.77 | 3.39 |
| | 8 | 2.17 | 71.69 | 34.23 | 21.68 | 0.937 | 247.02 | 269.43 | 4.61 | 4.23 |
| | 10 | 3.81 | 71.82 | 43.15 | 18.94 | 0.933 | 219.02 | 236.46 | 5.20 | 4.82 |
| 2.5 | 2 | 0.41 | 73.27 | 19.84 | 88.53 | 0.930 | 1090.89 | 1724.32 | 1.04 | 0.66 |
| | 4 | 0.69 | 71.16 | 22.22 | 51.26 | 0.910 | 644.71 | 823.49 | 1.77 | 1.38 |
| | 6 | 1.72 | 72.66 | 42.98 | 32.17 | 0.947 | 371.31 | 424.37 | 3.07 | 2.68 |
| | 8 | 1.81 | 71.89 | 27.76 | 24.74 | 0.931 | 283.44 | 313.35 | 4.02 | 3.64 |
| | 10 | 2.03 | 71.36 | 25.39 | 21.53 | 0.912 | 251.29 | 274.52 | 4.53 | 4.15 |

**Table 10**
THE VALUES OF CIRCUIT PARAMETERS AND ANODIC LAYER THICKNESSES OBTAINED FROM 0.1 M $H_2SO_4$ ELECTROLYTE USING EIS DATA

| j, mA | $E_f$, V | $Q_a$, mC | Rs, Ω | $R_{ox}$, MΩ | $Q_{ox}\cdot10^8$, $\Omega^{-1}s^{-n}$ | $n_{ox}$ | $C_{ox}$, nF | $C_a$, nF | $d_{ox}$, nm | $d_a$, nm |
|---|---|---|---|---|---|---|---|---|---|---|
| 0 | - | - | 20.67 | 2.55 | 459.69 | 0.937 | 5394.62 | - | 0.21 | - |
| 0.5 | 2 | 0.80 | 21.02 | 44.29 | 78.82 | 0.964 | 897.23 | 1076.23 | 1.27 | 1.06 |
| | 4 | 1.54 | 21.96 | 48.61 | 37.53 | 0.962 | 419.59 | 454.97 | 2.72 | 2.50 |
| | 6 | 2.94 | 21.17 | 108.36 | 29.80 | 0.954 | 351.98 | 376.55 | 3.24 | 3.03 |
| | 8 | 2.96 | 20.64 | 68.49 | 24.16 | 0.942 | 285.94 | 301.95 | 3.98 | 3.77 |
| | 10 | 3.63 | 21.67 | 205.20 | 18.07 | 0.956 | 213.09 | 221.85 | 5.35 | 5.14 |
| 1.0 | 2 | 0.66 | 21.99 | 34.21 | 121.65 | 0.948 | 1489.33 | 2057.30 | 0.77 | 0.55 |
| | 4 | 1.46 | 21.72 | 86.00 | 46.69 | 0.959 | 546.11 | 607.62 | 2.09 | 1.88 |
| | 6 | 2.17 | 22.65 | 104.78 | 30.52 | 0.958 | 354.02 | 378.88 | 3.22 | 3.01 |
| | 8 | 2.54 | 21.73 | 81.36 | 22.89 | 0.951 | 265.37 | 279.10 | 4.29 | 4.08 |
| | 10 | 2.25 | 20.82 | 73.83 | 17.73 | 0.939 | 208.67 | 217.06 | 5.46 | 5.25 |
| 2.5 | 2 | 0.68 | 21.36 | 22.06 | 119.34 | 0.948 | 1423.97 | 1934.64 | 0.80 | 0.59 |
| | 4 | 1.26 | 21.15 | 48.55 | 53.92 | 0.946 | 647.89 | 736.33 | 1.76 | 1.55 |
| | 6 | 1.63 | 21.05 | 56.78 | 28.46 | 0.937 | 341.32 | 364.37 | 3.34 | 3.13 |
| | 8 | 2.12 | 21.94 | 96.35 | 25.03 | 0.948 | 296.82 | 314.10 | 3.84 | 3.63 |
| | 10 | 2.43 | 21.50 | 60.86 | 22.18 | 0.932 | 266.62 | 280.49 | 4.27 | 4.06 |

**Table 11**
THE VALUES OF CIRCUIT PARAMETERS AND ANODIC LAYER THICKNESSES OBTAINED FROM 0.25 M $H_2SO_4$ ELECTROLYTE USING EIS DATA

| j, mA | $E_f$, V | $Q_a$, mC | Rs, Ω | $R_{ox}$, MΩ | $Q_{ox}\cdot10^8$, $\Omega^{-1}s^{-n}$ | $n_{ox}$ | $C_{ox}$, nF | $C_a$, nF | $d_{ox}$, nm | $d_a$, nm |
|---|---|---|---|---|---|---|---|---|---|---|
| 0 | - | - | 15.25 | 1.89 | 414.63 | 0.943 | 4677.15 | - | 0.24 | - |
| 0.5 | 2 | 0.71 | 15.64 | 38.11 | 813.47 | 0.950 | 972.33 | 1227.52 | 1.17 | 0.93 |
| | 4 | - | - | - | - | - | - | - | - | - |
| | 6 | - | - | - | - | - | - | - | - | - |
| | 8 | - | - | - | - | - | - | - | - | - |
| | 10 | - | - | - | - | - | - | - | - | - |
| 1.0 | 2 | 0.74 | 15.33 | 32.36 | 102.06 | 0.946 | 1240.04 | 1687.42 | 0.92 | 0.68 |
| | 4 | - | - | - | - | - | - | - | - | - |
| | 6 | - | - | - | - | - | - | - | - | - |
| | 8 | - | - | - | - | - | - | - | - | - |
| | 10 | - | - | - | - | - | - | - | - | - |
| 2.5 | 2 | 0.69 | 16.25 | 11.80 | 142.92 | 0.927 | 1775.60 | 2862.17 | 0.64 | 0.40 |
| | 4 | 1.88 | 15.83 | 30.05 | 38.16 | 0.953 | 428.91 | 472.21 | 2.66 | 2.41 |
| | 6 | 2.87 | 15.35 | 43.86 | 33.60 | 0.931 | 407.47 | 446.36 | 2.80 | 2.55 |
| | 8 | 2.50 | 15.32 | 30.01 | 20.62 | 0.928 | 236.06 | 248.60 | 4.83 | 4.58 |
| | 10 | 3.25 | 16.37 | 64.08 | 18.03 | 0.932 | 214.39 | 224.69 | 5.31 | 5.07 |

**Table 12**
THE VALUES OF CIRCUIT PARAMETERS AND ANODIC LAYER THICKNESSES OBTAINED FROM 0.5 M $HNO_3$ ELECTROLYTE USING EIS DATA

## Conclusions

The study of the niobia films is justified by the potential replacement stable oxide $Ta_2O_5$ with $Nb_2O_5$ as dielectric material for capacitors because the dielectric constant of niobia is higher than that of tantalum oxide. In addition, niobia has other applications in optoelectronics, the construction of solar cells, jewelry etc.

Open-circuit potential curves illustrate passive behavior of native niobia. EIS spectra of native film growth during two hours show capacitive features virtually identical for all forming potential for all solutions of acids used. Impedance modulus is kept constant at high frequency in a wide range. Differences occur in the spectra of native niobia formed in oxalic acid solutions, when semicircles are depressed and well defined. For the other two types of electrolytes (based on sulfuric and nitric acids) the recorded spectra present an arc close to the vertical axis, proving the formation of a solid electrically insulating film.

Cyclic voltammetry curves of niobium electrode polarization in all acid solutions are also characteristic for the formation of electrically insulating anodic films. There are however differences observed on anodic portions of the first cycle: unlike oxalic and nitric acid solutions, in sulfuric acid solutions in these areas appears a second region of increasing current, at polarization of 2-3 V/AgCl, after the current begins to decrease slowly again. Current jumps to the second region are broader in dilute solution (0.1 M $H_2SO_4$) to more concentrated solution (0.25 M $H_2SO_4$). This phenomenon could be explained by a transition of the niobium oxidation state, namely the gradual oxidation of Nb to $NbO_2$ continues to $Nb_2O_5$, which is the stable form. Dilute sulfuric acid solution also leads to a higher

concentration of niobium oxide intermediate in the form of tetravalent niobium $NbO_2$.

EIS spectra data allowed comparisons of influences of forming potential, forming current density and passivation media on the stability and behavior of niobia film capacitance.

Equivalent circuit modeling led to calculations of circuit parameters: resistance of the solution, the overall resistance of the interface and constant phase parameters. From these parameters it was possible to compute the total thickness of the grown oxide and the thickness of the anodized portion.

## References


1. DE SA, C. A. I. , RANGEL, M., SKELDON, P., THOMPSON, G.E., Semiconductive properties of anodic niobium oxides, in Portugaliae Electrochimica Acta, **24**, no. 2, 2006, pp. 305-311.

2. CHOI, J., HOON LIM, J., LEE, S. C., J. HO CHANG, J., KIM, K.J., CHO, M.A., Porous niobium oxide films prepared by anodization in HF/H3PO4, in Electrochimica Acta, **51**, 2006, pp. 5502–5507.

3. SKATKOV, L., LYASHOK, L., GOMOZOV, V., TOKAREV , I., ÂAYRACHNIY, B., Anodic formation of nanoporous crystalline niobium oxide, in Journal of Electrochemical Science Engineering, **4**, no. 2, 2014, pp. 75-83.

4. MANEA, A.C., ANICAI, L, Studies on the formation of zirconia films in some aqueous acidic solutions, in Rev. Chim. (Bucharest), **66**, no. 10, 2015, p. 1680

5. V. D. JOVIC AND B. M. JOVIC, Semiconducting properties of oxide films formed onto an Nb electrode in NaOH solutions, in J. Serb. Chem. Soc., **73**, no. 3, 2008, pp. 351-367.

6. M. R. S. ABOUZARI, F. BERKEMEIER, G. SCHMITZ AND D. WILMER, On the physical interpretation of constant phase elements, in Solid State Ionics, **180**, no. 14-16, Jun 25 2009, pp. 922-927



Manuscript received: 17.02.2015